PNAS
www.pnas.org

Supplementary Information for

Structures of the junctophilin – voltage-gated calcium channel interface reveal hot spot for cardiomyopathy mutations.

Zheng Fang Yang, Pankaj Panwar, Ciaran R. McFarlane, Wietske Elisabeth Tuinte, Marta Campiglio, Filip Van Petegem

Filip Van Petegem
Email: petegem@mail.ubc.ca

This PDF file includes:

Figures S1 to S6
Tables S1 to S8

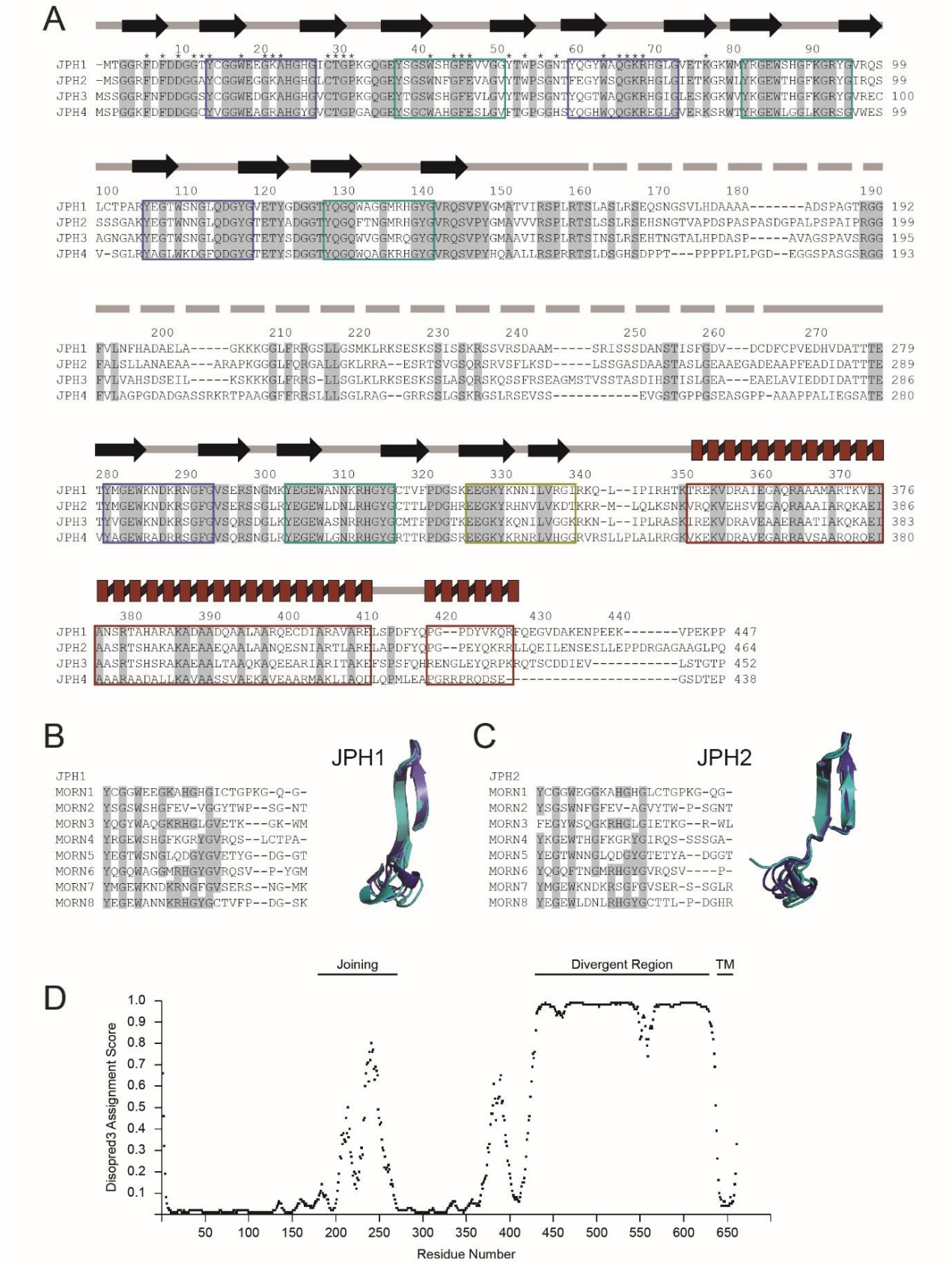
A
JPH1 -MTGGRFDFDDGGTYCGGWEEGKAHGHGICTGPKGQGEYSGSWSHGFEVVGGYTWPSGNTYQGYWAQGKRHGLGVETKGKWMYRGEWSHGFKGRYGVRQS 99
JPH2 -MSGGRFDFDDGGAYCGGWEGGKAHGHGLCTGPKGQGEYSGSWNFGFEVAGVYTWPSGNTFEGYWSQGKRHGLGIETKGRWLYKGEWTHGFKGRYGIRQS 99
JPH3 MSSGGRFNFDDGGSYCGGWEDGKAHGHGVCTGPKGQGEYTGSWSHGFEVLGVYTWPSGNTYQGTWAQGKRHGIGLESKGKWVYKGEWTHGFKGRYGVREC 100
JPH4 MSPGGKFDFDDGGQYVGGWEAGRAHGYGVCTGPGAQGEYSGCWAHGFESLGVFTGPGGHSYQGHWQQGKREGLGVERKSRWTYRGEWLGGLKGRSGVWES 99
JPH1 LCTPARYEGTWSNGLQDGYGVETYGDGGTYQGQWAGGMRHGYGVRQSVPYGMATVIRSPLRTSLASLRSEQSNGSVLHDAAAA-------ADSPAGTRGG 192
JPH2 SSSGAKYEGTWNNGLQDGYGTETYADGGTYQGQFTNGMRHGYGVRQSVPYGMAVVVRSPLRTSLSSLRSEHSNGTVAPDSPASPASDGPALPSPAIPRGG 199
JPH3 AGNGAKYEGTWSNGLQDGYGTETYSDGGTYQGQWVGGMRQGYGVRQSVPYGMAAVIRSPLRTSINSLRSEHTNGTALHPDASP-----AVAGSPAVSRGG 195
JPH4 V-SGLRYAGLWKDGFQDGYGTETYSDGGTYQGQWQAGKRHGYGVRQSVPYHQAALLRSPRRTSLDSGHSDPPT---PPPPLPLPGD--EGGSPASGSRGG 193
JPH1 FVLNFHADAELA-----GKKKGGLFRRGSLLGSMKLRKSESKSSISSKRSSVRSDAAM-----SRISSSDANSTISFGDV---DCDFCPVEDHVDATTTE 279
JPH2 FALSLLANAEAA---ARAPKGGGLFQRGALLGKLRRA--ESRTSVGSQRSRVSFLKSD-----LSSGASDAASTASLGEAAEGADEAAPFEADIDATTTE 289
JPH3 FVLVAHSDSEIL-----KSKKKGLFRRS-LLSGLKLRKSESKSSLASQRSKQSSFRSEAGMSTVSSTASDIHSTISLGEA---EAELAVIEDDIDATTTE 286
JPH4 FVLAGPGDADGASSRKRTPAAGGFFRRSLLLSGLRAG--GRRSSLGSKRGSLRSEVSS----------EVGSTGPPGSEASGPP-AAAPPALIEGSATE 280
JPH1 TYMGEWKNDKRNGFGVSERSNGMKYEGEWANNKRHGYGCTVFPDGSKEEGKYKNNILVRGIRKQ-L--IPIRHTKTREKVDRAIEGAQRAAAMARTKVEI 376
JPH2 TYMGEWKNDKRSGFGVSERSSGLRYEGEWLDNLRHGYGCTTLPDGHREEGKYRHNVLVKDTKRR-M--LQLKSNKVRQKVEHSVEGAQRAAAIARQKAEI 386
JPH3 TYVGEWKNDKRSGFGVSQRSDGLKYEGEWASNRRHGYGCMTFPDGTKEEGKYKQNILVGGKRKN-L--IPLRASKIREKVDRAVEAAERAATIAKQKAEI 383
JPH4 VYAGEWRADRRSGFGVSQRSNGLRYEGEWLGNRRHGYGRTTRPDGSREEGKYKRNRLVHGGRVRSLLPLALRRGKVKEKVDRAVEGARRAVSAARQRQEI 380
JPH1 ANSRTAHARAKADAADQAALAARQECDIARAVARELSPDFYQPG--PDYVKQRFQEGVDAKENPEEK-------VPEKPP 447
JPH2 AASRTSHAKAKAEAAEQAALAANQESNIARTLARELAPDFYQPG--PEYQKRRLLQEILENSESLLEPPDRGAGAAGLPQ 464
JPH3 AASRTSHSRAKAEAALTAAQKAQEEARIARITAKEFSPSFQHRENGLEYQRPKRQTSCDDIEV-----------LSTGTP 452
JPH4 AAARAADALLKAVAASSVAEKAVEAARMAKLIAQDLQPMLEAPGRRPRQDSE----------------------GSDTEP 438
B
JPH1
JPH1
MORN1 YCGGWEECGKAHGHGICTGPKG-Q-G-
MORN2 YSGSWSHGFEV-VGGYTWP--SG-NT
MORN3 YQGYWAQGKRHGLGVETK---GK-WM
MORN4 YRGEWSHGFKGRYGVRQS--LCTPA-
MORN5 YEGTWSNGLQDGYGVETYG--DG-GT
MORN6 YQGQWAGGMRHGYGVRQSV--P-YGM
MORN7 YMGEWKNDKRNGFGVSERS--NG-MK
MORN8 YEGEWANNKRHGYGCTVFP--DG-SK
C
JPH2
JPH2
MORN1 YCGGWEGGKAHGHGLCTGPKG-QG-
MORN2 YSGSWNFGFEV-AGVYTW-P-SGNT
MORN3 FEGYWSQGKRHGLGIETKG--R-WL
MORN4 YKGEWTHGFKGRYGIRQS-SSSGA-
MORN5 YEGTWNNGLQDGYGTETYA--DGGT
MORN6 YQGQFTNGMRHGYGVRQSV----P-
MORN7 YMGEWKNDKRSGFGVSER-S-SGLR
MORN8 YEGEWLDNLRHGYGCTTL-P-DGHR
D
Joining
Divergent Region
TM
Disopred3 Assignment Score
1.0
0.9
0.8
0.7
0.6
0.5
0.4
0.3
0.2
0.1
50
100
150
200
250
300
350
400
450
500
550
600
650
Residue Number

Fig. S1. Sequence alignments (A) The sequence alignment of the N-terminal region of human JPH1-JPH4, with conserved residues between all 4 isoforms highlighted in grey. The deleted linker region in JPH1 and JPH2 are shown in dashes. The secondary elements of the crystal structures are shown above the sequences, while the MORN consensus sequences are boxed in the same colors as Figure 1A-C. JPH2 residues within 4.5Å from the $Ca_V1.1$ peptide in the co-crystal structure are starred above the sequences. Most of these are conserved among all JPH isoforms. The Uniprot IDs for the aligned sequences are: JPH1: Q9HDC5; JPH2: Q9BR39; JPH3: Q8WXH2; JPH4: Q96JJ6. (B) and (C) the structure-based sequence alignments of the 8 MORN repeats from JPH1 and JPH2, along with a structural superposition of these repeats, showing a remarkable structural similarity. (D) The Disopred3 plot of the full JPH1 sequence, with higher values corresponding to higher likelihood of being intrinsically disordered.

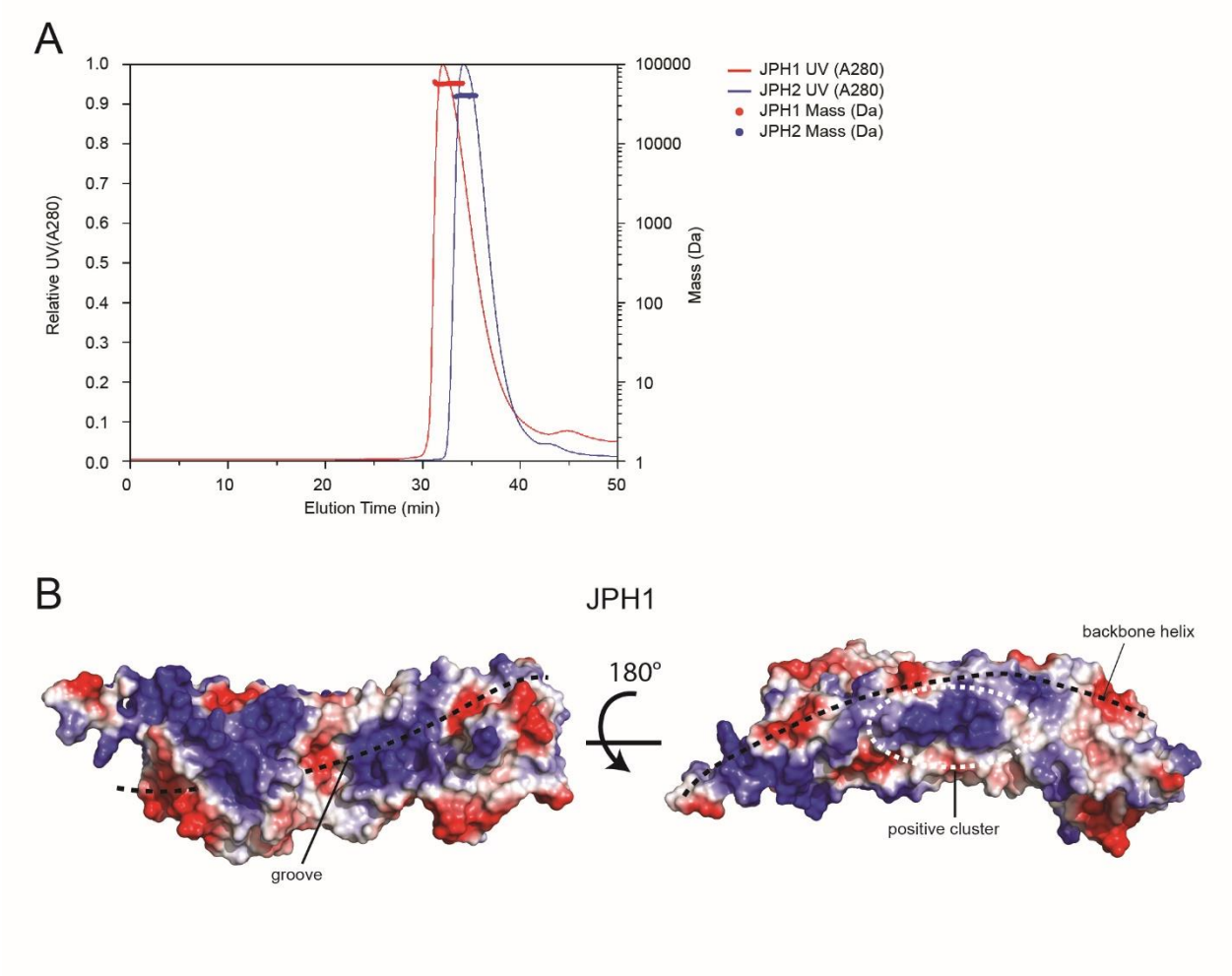

Fig. S2. Size and charge profile of Junctophilin. (**A**) The elution profile of JPH1 and JPH2 MORN-helical domain and predicted molecular weight based on SEC-MALS. Values are reported in table S3. Based on sequence, the expected molecular weight for a JPH1(1-442) containing a C-terminal strep tag is 49.8 kDa; the expected molecular weight of JPH2(1-437) is 47.2kDa. The SEC chromatogram and the estimated molecular weight based on light scattering for JPH1 and JPH2 are shown in red and blue respectively, which suggest monomeric forms for both in solution. (**B**) Surface electrostatic potential generated for JPH1 in 2 orientations, similar to Figure 1D,E for JPH2.

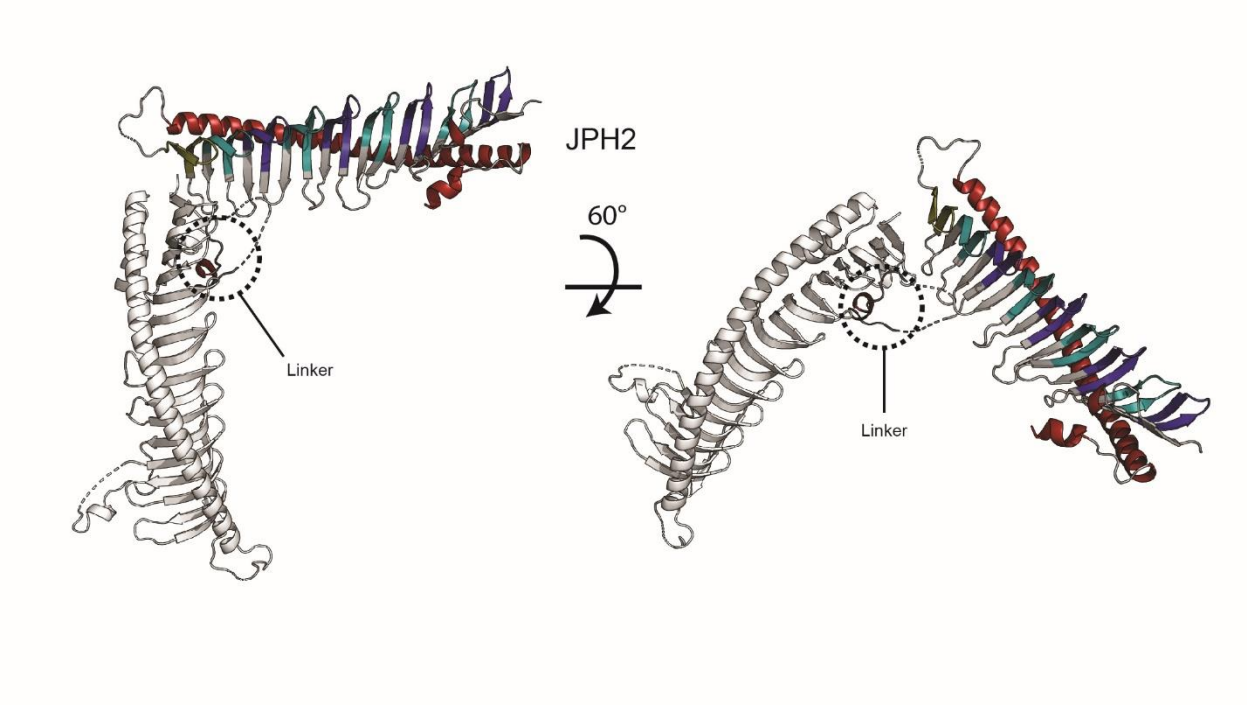

Fig. S3. The shortened linker of JPH2 forms crystal contacts with a neighboring asymmetric unit. One asymmetric unit of JPH2 is colored according to Figure 1A-C, the shortened linker region is colored in black and interacts with a neighboring asymmetric unit which is colored in white. Regardless of this observed crystal contact, no dimeric interactions are observed via SEC-MALS, so this likely only arises in the context of the crystal.

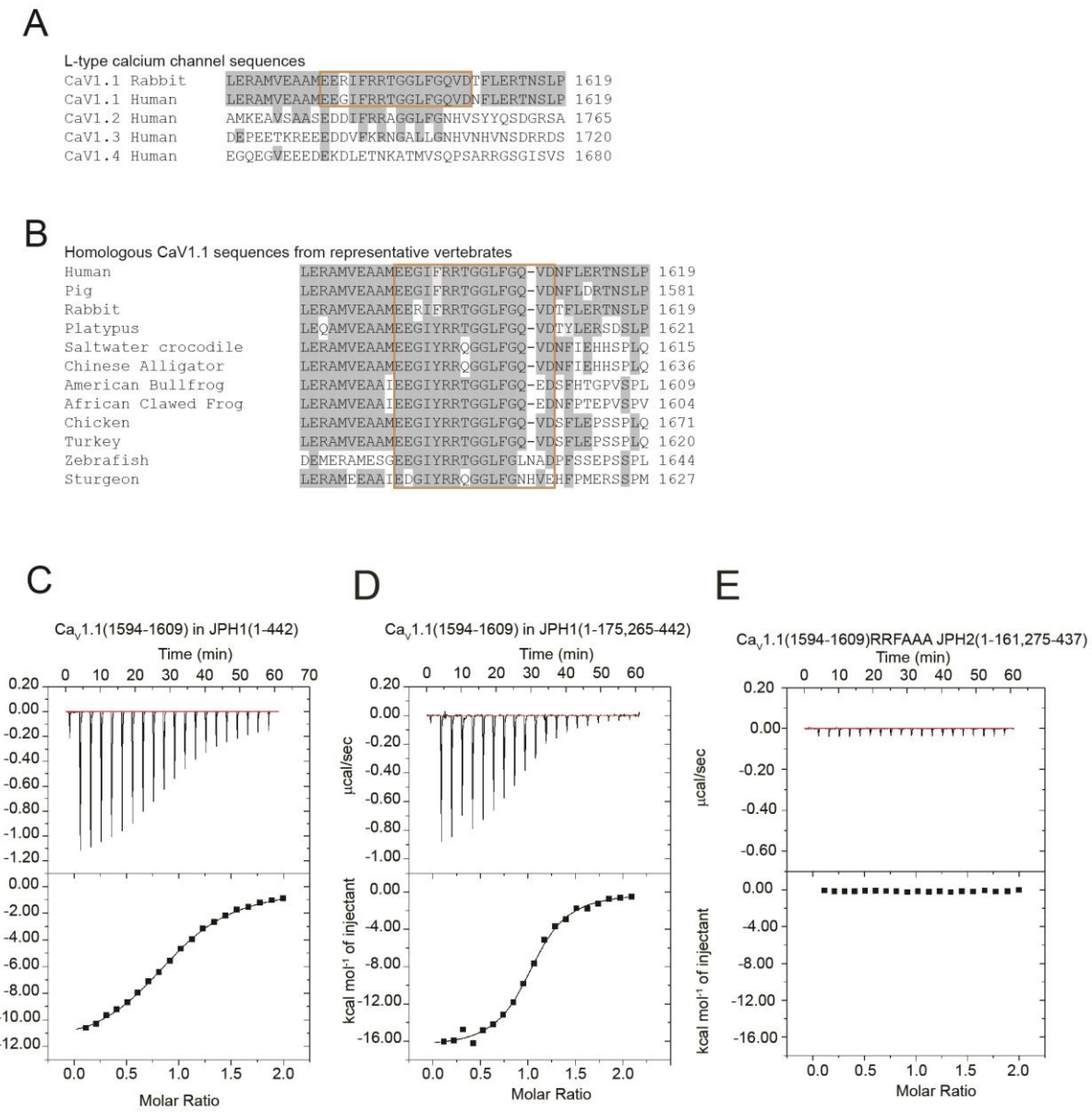

Fig. S4: The sequence alignments of rabbit $Ca_V1.1$ and human $Ca_V1.1$-1.4, and sequence alignments of $Ca_V1.1$ from diverse vertebrates. (**A**) Rabbit $Ca_V1.1$ and human $Ca_V1.1$-1.4 sequences are aligned with Clustal Omega, and the interaction site with JPH is shown (orange box) with 10 upstream and downstream residues. Conserved residues to rabbit $Ca_V1.1$ are highlighted in grey. The Uniprot IDs for the aligned sequences are: r$Ca_V1.1$: P07293; h$Ca_V1.1$: Q13698; h$Ca_V1.2$: Q13936; h$Ca_V1.3$: Q01668; h$Ca_V1.4$: O60840. (**B**) $Ca_V1.1$ sequences from 12 representative vertebrates are aligned with Clustal Omega, and the peptide interacting with JPHs is shown (orange box), along with 10 upstream and downstream residues. Conserved residues are highlighted in grey. The Uniprot IDs for the $Ca_V1.1$ sequences are: human: Q13698; rabbit: P07293; pig: A0A5G2QW60; platypus: F7DM66; saltwater crocodile: A0A7M4EDG7; Chinese alligator: A0A3Q0FSH7; American bullfrog: O57483; African clawed frog: A0A1L8H6Q1; chicken: A0A1D5PV02; turkey: G1MQJ3; zebrafish: Q6RKB0; sturgeon: E7EAV0. (**C**) ITC of 600 µM $Ca_V1.1$ peptide into 60 µM JPH1 (1-442) containing the joining region (K_d =7.9 µM). (**D**) ITC of 300 µM $Ca_V1.1$ peptide into 28 µM JPH1 (1-175, 265-442) lacking most of the joining region (K_d = 1.1µM) (**E**) ITC of 300 µM RRF/AAA mutant $Ca_V1.1$ peptide into 30 µM JPH2 (1-161,275-437), showing no significant heats different from background.

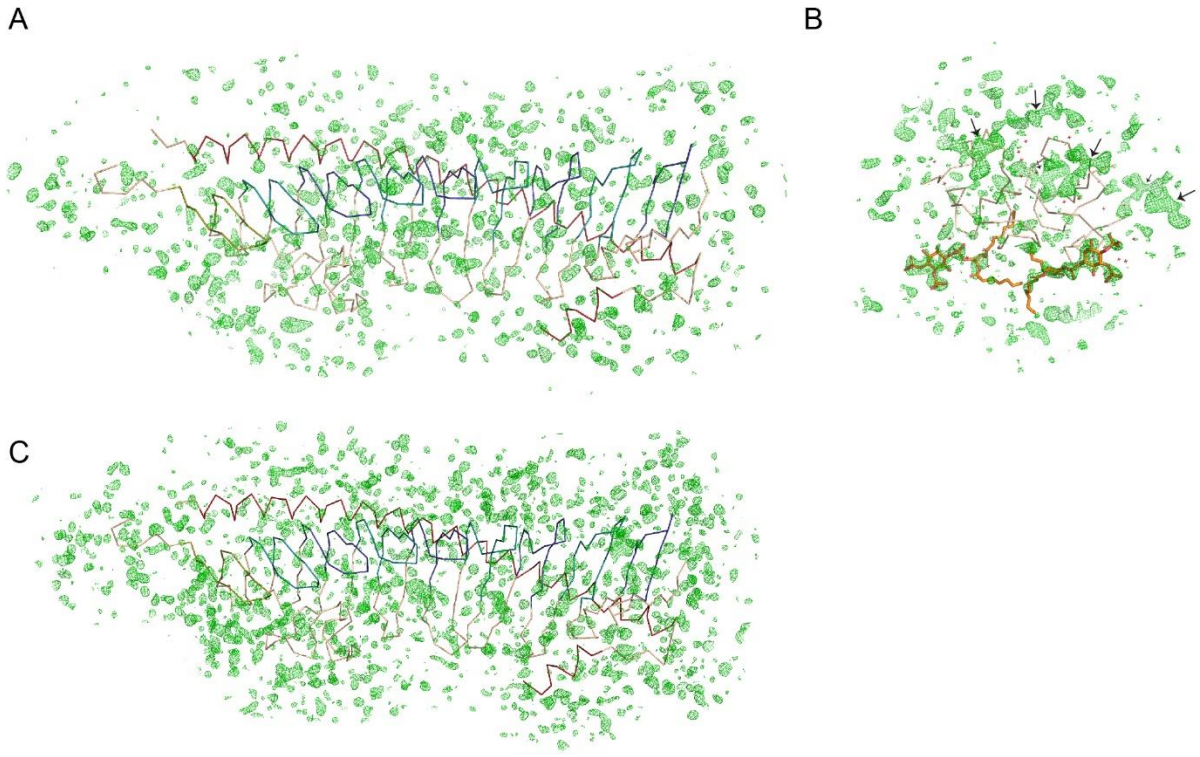

Fig. S5: **Absence of density for lipids in JPH1 crystals.** (**A**) Fo-Fc difference density map (green) for a 2.0Å dataset of a JPH1 crystal grown in the presence of 500μM 8:0 PI(4,5)P_2. The map is contoured at 2.5σ, with the model of JPH1 shown in Cα trace. Even at this threshold, only noise peaks are visible. (**B**) Reference Fo-Fc difference density map for 8:0 PI(4,5)P_2 bound to human β-defensin 2 (PDB ID 6CS9). The difference map was generated after removal of PIP2 from the model, and contoured at 2.5σ. The ribbon represents a Cα trace model of the protein, with the sticks indicating two PIP2 molecules. Electron densities for symmetry-related PIP2 molecules are also visible above (arrows). The zoom level is the same as in panel A, showing that similar densities are not observed for JPH1. (**C**) Fo-Fc difference density map (green) for a 1.9Å dataset of JPH1 crystal grown in the presence of 2mM 6:0 phosphatidylserine, contoured at 2.5σ. No density is observed that could readily fit a phosphatidylserine.

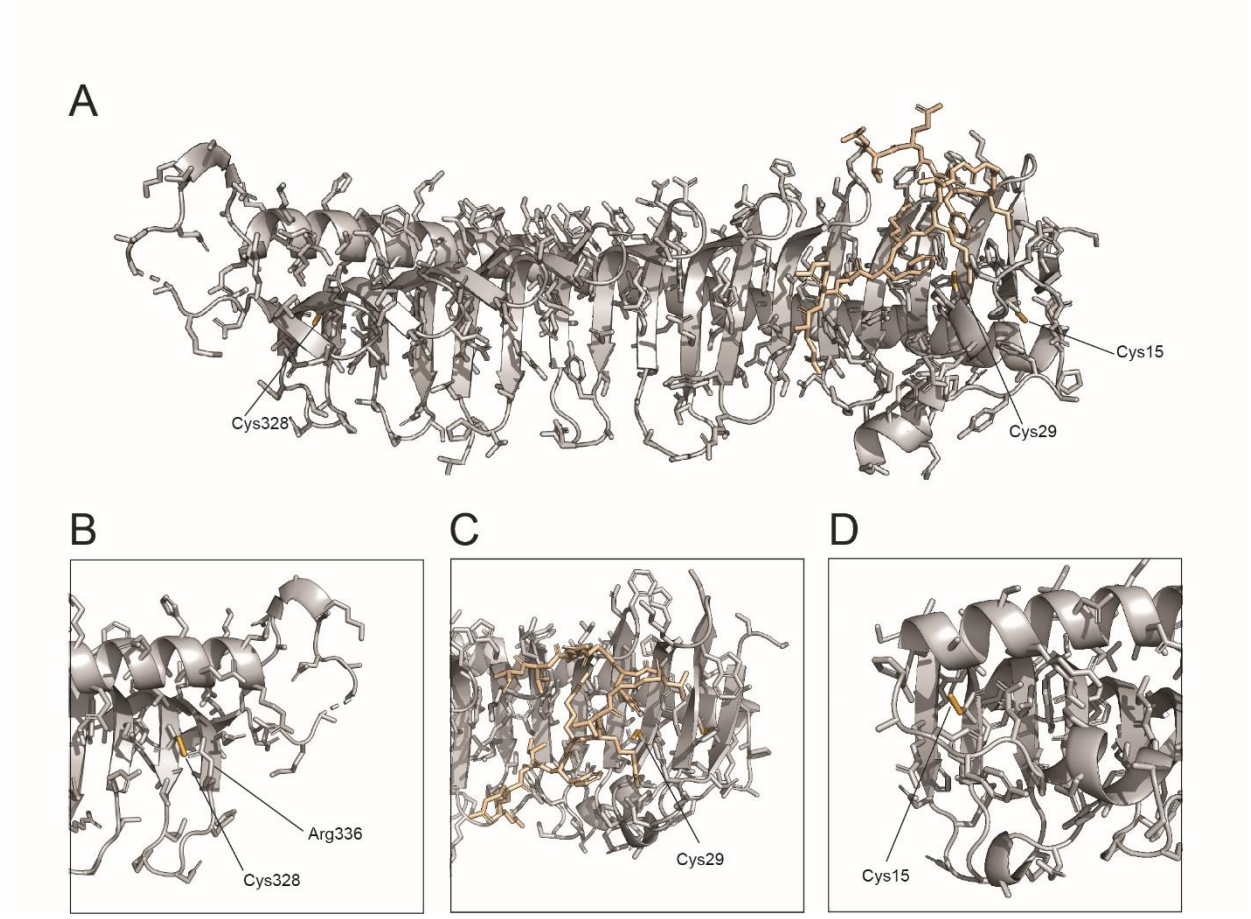

Fig. S6: Potential palmitoylation sites on JPH2 are inaccessible. (**A**) The JPH2 crystal structure with 3 potential palmitoylation sites: Cys15, Cys29, and Cys328. Cysteine sidechains are colored in orange; the $Ca_V1.1$ peptide is colored in beige. (**B**) Cys328 is buried by Arg336 and thus inaccessible with a calculated solvent accessible area of 0.0 $Å^2$ for the sulfhydryl group. (**C**) In the absence of a $Ca_V1.1$ peptide, the Cys29 sulfhydryl has a solvent accessible area of 25 $Å^2$, which reduces to 9.8 $Å^2$ in the presence of the peptide. The presence of the peptide leaves no space for a bulky palmitate group (**D**) Cys15 is buried by the backbone α-helix with a solvent accessible area of 0.0 $Å^2$. Contact areas are calculated with AREAIMOL in CCP4 with a probe solvent molecule with radius 1.4 Å.

Table S1 Data collection, phasing and refinement statistics for JPH1 data

	Native JPH1 (PDB 7RW4)	Se-Met JPH1
Data collection		
Space group	$P2_12_12_1$	$P2_12_12_1$
Cell dimensions		
a, *b*, *c* (Å)	44.08, 55.20, 142.45	44.08, 55.20, 142.45
α, β, γ (°)	90, 90, 90	90, 90, 90
Wavelength (Å)	0.97937	0.97937
Resolution (Å)	40.00-1.31 (1.34-1.31)	40.00-1.65 (1.69-1.65)
R_{merge}	0.073 (1.097)	0.065 (0.763)
R_{pim}	0.031 (0.542)	0.036 (0.448)
CC½	0.995 (0.502)	0.994 (0.619)
I / σ*I*	23.96 (1.50)	18.35 (2.17)
Completeness (%)	92.29 (33.27)	99.21 (96.02)
Redundancy	6.3 (5.0)	3.8 (3.5)
Refinement		
Resolution (Å)	37.48-1.31	
No. reflections	77976	
R_{work} / R_{free}	0.1366 / 0.1680	
No. atoms		
Protein	2496	
Ligand/ion	40	
Water	327	
B-factors		
Protein	18.31	
Ligand/ion	42.11	
Water	33.72	
R.m.s deviations		
Bond lengths (Å)	0.012	
Bond angles (°)	1.23	

*Values in parentheses are for highest-resolution shell.

Table S2 Data collection and refinement statistics (molecular replacement)

	Apo-JPH2 (PDB 7RXE)	JPH2-Ca_V peptide complex (PDB 7RXQ)
Data collection		
Space group	$P3_221$	C2
Cell dimensions		
a, *b*, *c* (Å)	63.121, 63.121, 149.68	116.39, 30.38, 96.68
α, β, γ (°)	90, 90, 120	90, 115.96, 90
Wavelength (Å)	0.97946	0.97946
Resolution (Å)	54.66-2.35 (2.48-2.35)	44.34-2.03 (2.07-2.03)
R_{merge}	0.295 (1.435)	0.052 (0.225)
R_{pim}	0.105 (0.496)	0.034 (0.149)
CC½	0.983 (0.371)	0.998 (0.950)
$I / \sigma I$	5.4 (1.5)	13.3 (1.8)
Completeness (%)	100.0 (100.0)	97.10 (97.71)
Redundancy	8.7 (9.2)	3.2 (3.2)
Refinement		
Resolution (Å)	36.85–2.35	38.07–2.03
No. reflections	14993	19586
R_{work} / R_{free}	0.2175 / 0.2606	0.2024 / 0.2517
No. atoms		
Protein	2411	2165
Ligand/ion	38	18
Water	93	127
B-factors		
Protein	37.98	44.12
Ligand/ion	43.53	57.39
Water	36.78	38.08
R.m.s. deviations		
Bond lengths (Å)	0.006	0.007
Bond angles (°)	0.86	0.90

*Values in parentheses are for highest-resolution shell.

Table S3: Estimated molecular weight of JPH1 and JPH2 based on size-exclusion chromatography (SEC) and multi-angle light scattering (MALS).

Construct	Estimated molecular weight based on SEC (kDa)	Estimated molecular weight based on MALS (kDa)	Molecular weight based on protein sequence (kDa)
JPH1(1-442)	51.9	56.8	49.8
JPH1(1-161,265-442)	32.4	35.0	37.9
JPH2(1-437)	48.9	40.1	47.2
JPH2(1-161,275-437)	35.6	33.5	36.1

Table S4. Affinity values for the binding between junctophilin MORN-helix domains and the CTD constructs of $Ca_V1.1$

Titrated constructs	K_d, μM	N value	ΔH, kcal $\cdot mol^{-1}$	ΔS, kcal $\cdot mol^{-1}K^{-1}$	No of replicates
$Ca_V1.1$ 1594-1609/ JPH1 1-442	7.7 ± 0.3	0.9 ± 0.1	-12.5 ± 1.0	-18.7 ± 3.2	3
$Ca_V1.1$ 1594-1609/ JPH1 1-175,265-442	1.1 ± 0.2	0.9 ± 0.1	-16.7 ± 0.3	-28.7 ± 1.4	3
$Ca_V1.1$ 1594-1609/ JPH2 1-161,275-437	1.7 ± 0.3	1.0 ± 0.1	-15.8 ± 0.7	-26.6 ± 2.6	3
$Ca_V1.1$ 1594-1609/ MBP-JPH2 1-161,275-437	1.8 ± 0.2	0.99 ± 0.02	-16.9 ± 0.4	-30.2 ± 1.4	3
$Ca_V1.1$ 1594-1609/ MBP-JPH2 1-161,275-437(E47A)	25.3 ± 3.5	1.0 ± 0.1	-14.3 ± 0.5	-27.0 ± 1.9	3

Table S5. $Ca_V1.1$ conductance and calcium transient parameters

	Ca^{2+} current parameters		
Parameter	**$Ca_V1.1$**	**$Ca_V1.1$-RRFAAA**	**p-value**
I_{peak} (pA/pF)	-2.29 ± 0.33	-1.78 ± 0.28	0.2708
V_{rev} (mV)	82.59 ± 1.99	82.22 ±2.26	0.9104
$V_{1/2}$ (mV)	26.18 ± 1.09	26.41 ± 4.5	0.9652
G_{max} (nS/nF)	63.85 ± 8.01	54.97 ± 8.64	0.4867
K_{act} (mV)	9.25 ± 0.32	11.28 ± 1.31	0.1999
n	10	12	-
	Ca^{2+} transients parameters		
Parameter	**$Ca_V1.1$**	**$Ca_V1.1$-RRFAAA**	**p-value**
$\Delta F/F_{max}$	0.92 ± 0.17	0.52 ± 0.07	0.0385
V_F (mV)	5.76 ± 2.16	5.87 ± 2.33	0.9744
K_F (mV)	7.43 ± 1.06	5.76 ± 0.65	0.2001
n	10	12	-

Average values of parameters obtained by fits of equations 1 and 2 (Material and methods) to I-V and ΔF/F-V data, respectively. Data are expressed as mean ± S.E. p-values are from Student t-test.

Table S6. Sequence Variants in Junctophiln-2, obtained from Clinvar and peer-reviewed literature. All H-bonds were determined via HBPLUS

Sequence variant	Disease phenotype	Location of mutation	Reference, if available	Predicted effect
G3E	Not provided	1st β-strand		G3 occupies a location on the Ramachandran plot only allowed for Gly
G20R	Primary familial hypertrophic cardiomyopathy	MORN 1		Surface residue change
G21E	Hypertrophic cardiomyopathy	MORN1 (MORN consensus residue G8)		Surface residue change
G31D	Hypertrophic cardiomyopathy	MORN1		Surface residue change
K33R	Hypertrophic cardiomyopathy	MORN1		Surface residue change
N43S	Cardiovascular phenotype, not specified, Hypertrophic cardiomyopathy, Familial hypertrophic cardiomyopathy 17	MORN2		Surface residue change
E47A	Hypertrophic cardiomyopathy	MORN2		Affects packing against W42 in MORN2 and W64 in MORN3; affects salt bridge with CaV1.1 residue R1599
P55A	Hypertrophic cardiomyopathy	MORN2	De Bruijn et al(1)	Affects packing against residue Y433 in backbone α-helix
P55L	Hypertrophic cardiomyopathy	MORN2		Affects packing against residue Y433 in backbone α-helix
G57R	Not provided	MORN2		G57 occupies location on Ramachandran plot only allowed for Gly
W64*	Familial hypertrophic cardiomyopathy 17	MORN3 (MORN consensus residue W5)		Premature stop codon; truncated product
I74V	Hypertrophic cardiomyopathy	MORN3		Affects packing against E402 in backbone α-helix
T76A	Not provided, Familial hypertrophic cardiomyopathy 17	MORN3		Surface residue change
K77E	Hypertrophic cardiomyopathy	MORN3		Affects salt bridge with E75; affects salt bridge with $Ca_V1.1$ residue E1595
R93H	Primary dilated cardiomyopathy, not provided	MORN4		Affects packing against T109; affects H-bond with W110 carbonyl oxygen
R97W	Hypertrophic cardiomyopathy	MORN4		Affects H-bond with Q115

R97Q	Hypertrophic cardiomyopathy	MORN4		Affects H-bond with Q115
S100L	Not provided	MORN4		Affects H-bond with G78 carbonyl oxygen
S101R	Familial hypertrophic cardiomyopathy 17	MORN4	Landstrom et al(2) Bennett et al(3)	Surface residue change
G103S	Hypertrophic cardiomyopathy	MORN4		Surface residue change
G117C	Hypertrophic cardiomyopathy	MORN5 (MORN Consensus residue G12)		G117 occupies a location in the Ramachandran plot only allowed for Gly
E121K	Hypertrophic cardiomyopathy	MORN5		Affects H-bond with Q115 and H-bond with Y123
G126R	Not specified	MORN5		G126 occupies a location in the Ramachandran plot only allowed for Gly
Y129D	Not specified, Hypertrophic cardiomyopathy	MORN6 (MORN consensus residue Y1)		Affects H-bond with Q132 mainchain and H-bond with Y141 carbonyl oxygen; affects packing against R138
G136S	Hypertrophic cardiomyopathy	MORN6 (MORN consensus residue G8)		Surface residue change
R138S	Not provided	MORN6		Affects H-bond with Y123 and H bond with D298 carbonyl oxygen; affects packing against Y129
Y141H	Familial hypertrophic cardiomyopathy 17, Familial hypertrophic cardiomyopathy 1	MORN6	Landstrom et al(2) Woo et al(4)	Affects packing against D294 and I379 of backbone α-helix
G142*	Not provided	MORN6 (MORN consensus residue G14)		Premature stop codon leading to truncated product
S146G	Hypertrophic cardiomyopathy	MORN6		Affects H-bond with V147 carbonyl oxygen
S146R	Familial hypertrophic cardiomyopathy 1	MORN6		Affects H-bond with V147 carbonyl oxygen
V147M	Hypertrophic cardiomyopathy	MORN6		Surface residue change
P148L	Hypertrophic cardiomyopathy, Not provided	MORN6		Surface residue change
G150R	Not provided, Hypertrophic cardiomyopathy	MORN6		Surface residue change
V153A	Not specified, not provided, Familial hypertrophic cardiomyopathy 17, Hypertrophic cardiomyopathy	Joining region		Surface residue change

R156C	Hypertrophic cardiomyopathy	Joining region		Surface residue change
P158L	Hypertrophic cardiomyopathy	Joining region		Surface residue change
L159Q	Cardiovascular phenotype, Hypertrophic cardiomyopathy	Joining region		Surface residue change
T161K	Primary familial hypertrophic cardiomyopathy, Hypertrophic cardiomyopathy	Joining region	Vanninen et al(5)	Affects H-bond with P158 carbonyl oxygen
A277S	Hypertrophic cardiomyopathy	Joining region		Surface residue change
P278R	Hypertrophic cardiomyopathy	Joining region		Surface residue change
E280K	Cardiovascular phenotype, not specified, Familial hypertrophic cardiomyopathy 17	Joining region		Surface residue change
A285D	Hypertrophic cardiomyopathy	Joining region		Surface residue change
T290I	Hypertrophic cardiomyopathy	Joining region		Affects H-bond with Q145; change in hydrophobicity at the surface
T290S	Hypertrophic cardiomyopathy	Joining region		Thr290 forms a H-bond with Q145; Ser290 may form the same H-bond
M292T	Hypertrophic cardiomyopathy	MORN7		Affects packing against V143 and R381 of backbone helix
K296T	Hypertrophic cardiomyopathy	MORN7		Surface residue change
R300P	Hypertrophic cardiomyopathy	MORN7		Affects ionic interaction with E289 and H-bond with N321
S306G	Familial hypertrophic cardiomyopathy 17	MORN7		Affects polar interaction with E289
E307K	Not provided	MORN7		Surface residue change
E315K	Cardiovascular phenotype	MORN8		Affects salt bridge, causing repulsion with R313; affects H-bond with Q374 of backbone α-helix
E315G	Not provided	MORN8		Affects salt bridge, causing repulsion with R313; affects H-bond with Q374 of backbone α-helix
E317K	Hypertrophic cardiomyopathy	MORN8		Affects H-bond with Y326 amide nitrogen and S369 of backbone α-helix
R323H	Not provided	MORN8		Affects H-bond with T329 and H-bond with N344

T329A	Not provided	MORN8		Affects H-bond with R323 and H bond with Y341
T329N	Hypertrophic cardiomyopathy	MORN8		Affects H-bond with R323 and H bond with Y341
G339S	Cardiovascular phenotype, Hypertrophic cardiomyopathy	Pseudo MORN		G339 occupies a location in the Ramachandran plot only allowed for Gly
V345L	Hypertrophic cardiomyopathy	Pseudo MORN		Surface residue change
R353C	Hypertrophic cardiomyopathy	Loop		Surface residue change
N360H	Familial hypertrophic cardiomyopathy 17, not provided	Loop		Affects H-bond with K365 of backbone α helix
K361N	Hypertrophic cardiomyopathy	Loop		Surface residue change
Q364*	Not provided, not specified	Backbone α helix		Premature stop codon leading to truncated product
S369T	Hypertrophic cardiomyopathy	Backbone α helix		Affects H-bond with E317 in MORN8; affects H-bond with K365 and V366 carbonyl oxygens in backbone α-helix
R375C	Hypertrophic cardiomyopathy	Backbone α-helix		Surface residue change
R381C	Hypertrophic cardiomyopathy	Backbone α-helix		Affects packing against M292 in MORN7
K383N	Not provided	Backbone α-helix		Surface residue change
S392N	Hypertrophic cardiomyopathy	Backbone α-helix		Surface residue change
A394T	Hypertrophic cardiomyopathy	Backbone α-helix		Alanine residue facing glycine valley formed by the MORN repeats; possible steric hindrance for a larger residue.
E402K	Familial hypertrophic cardiomyopathy 17, not specified, not provided, Hypertrophic cardiomyopathy, Primary familial hypertrophic cardiomyopathy	Backbone α-helix		Affects salt bridge with K83 in MORN4
Q403E	Hypertrophic cardiomyopathy	Backbone α-helix		Surface residue change
A405S	Hypertrophic cardiomyopathy Basal septal hypertrphic and diastolic dysfunction	Backbone α-helix	Beavers et al(6) Quick et al(7)	Alanine residue facing glycine valley formed by the MORN repeats; possible steric hindrance for any larger residue
A405T	Familial hypertrophic cardiomyopathy 17,	Backbone α-helix	Seidelmann et al(8)	Alanine residue facing glycine valley formed by the

	Hypertrophic cardiomyopathy, Cardiovascular phenotype			MORN repeats; possible steric hindrance for any larger residue
A407D	Hypertrophic cardiomyopathy	Backbone α-helix		Surface residue change
N409K	Primary dilated cardiomyopathy	Backbone α-helix		Affects H-bond with E61 in MORN3 and H-bond with A405 carbonyl oxygen
S412C	Hypertrophic cardiomyopathy	Backbone α-helix		Affects H-bond with S39 in MORN2
I414L	Idiopathic dilated cardiomyopathy (DCM)	Backbone α-helix	Miura et al(9)	Affects packing against H26 in MORN1
I414V	Not provided	Backbone α-helix		Affects packing against H26 in MORN1
R416C	Not provided	Backbone α-helix		Affects salt bridge with E37 in loop between MORN1-2; affects H-bond with N413 of backbone helix
A423S	Hypertrophic cardiomyopathy	Loop		Residue at the interface with MORN repeats
P424L	Hypertrophic cardiomyopathy	Loop		Surface residue change
Q428*	Primary dilated cardiomyopathy	Loop		Premature stop codon leading to truncated product
P431L	Not provided	Short helix		Surface residue change
R436C	Hypertrophic cardiomyopathy	Short helix	Matsushita et al(10)	Surface residue change

Table S7
Human $Ca_V1.1$ sequence variants in the junctophilin interaction domain, obtained from the Clinvar and gnomAD databases.

Mutation	Disease	Source	Allele Frequency	Predicted effect
F1598L	Not provided	gnomAD	3.98e-6	Affects packing against JPH2 residue P32
R1599P	Not provided	gnomAD	6.38e-5	Affects H-bond with JPH2 residue G45 carbonyl oxygen and salt bridge with E47; affects intra-chain H-bond with G1606 carbonyl
R1599Q	Not provided	gnomAD	2.48e-5	Affects H-bond with JPH2 residue G45 carbonyl oxygen and salt bridge with JPH2 residue E47; affects intra-chain H-bond with G1606 carbonyl oxygen
R1599W	Malignant hyperthermia, susceptibility to, 5, Hypokalemic periodic paralysis 1	Clinvar	3.19e-5	Affects H-bond with JPH2 residue G45 carbonyl oxygen and salt bridge with JPH2 residue E47; affects intra-chain H-bond with G1606 carbonyl oxygen
G1603A	Not provided	gnomAD	4.00e-6	G1603 occupies a location in the Ramachandran plot only allowed for Gly
L1604M	Not provided	Clinvar	1.20e-5	Affects packing against JPH2 residues Y14 and W18
G1606A	Not Provided	gnomAD	3.99e-6	G1606 occupies a location in the Ramachandran plot only allowed for Gly

Table S8
Human $Ca_V1.2$ sequence variants in the junctophilin interaction domain, obtained from the Clinvar and gnomAD databases. Given the similarity with the corresponding region in CaV1.1, the predicted effects are based on the assumption that these corresponding residues are involved in similar interactions as observed in the JPH2-CaV1.1 crystal structure.

Mutation	Disease	Source	Allele frequency	Predicted effect
I1743T	Long QT Syndrome	Clinvar	4.01e-6	Affects packing against JPH2 residues Y52, W54, and W64
R1745M	Not provided	gnomAD	4.02e-6	Affects H-bond with JPH2 residue G45 carbonyl oxygen and salt bridge with JPH2 residue E47; affects intra-chain H-bond with G1752 carbonyl oxygen
G1748S	Long QT Syndrome; Brugada syndrome 3, Timothy syndrome	Clinvar	5.43e-5	G1748S occupies a location in the Ramachandran plot only allowed for Gly
G1752S	Long QT Syndrome	Clinvar	9.47e-6	Affects packing against JPH2 residue F46
H1754D	Not provided	gnomAD	4.53e-6	Surface residue change

SI References

1. S. De Bruijn *et al.*, A special case of hypertrophic cardiomyopathy with a differential diagnosis of isolated cardiac amyloidosis or junctophilin type 2 associated cardiomyopathy. *Acta clinica Belgica* **76**, 136-143 (2021).
2. A. P. Landstrom *et al.*, Mutations in JPH2-encoded junctophilin-2 associated with hypertrophic cardiomyopathy in humans. *Journal of molecular and cellular cardiology* **42**, 1026-1035 (2007).
3. H. J. Bennett *et al.*, Human junctophilin-2 undergoes a structural rearrangement upon binding PtdIns(3,4,5)P3 and the S101R mutation identified in hypertrophic cardiomyopathy obviates this response. *The Biochemical journal* **456**, 205-217 (2013).
4. J. S. Woo *et al.*, Hypertrophy in skeletal myotubes induced by junctophilin-2 mutant, Y141H, involves an increase in store-operated Ca2+ entry via Orai1. *The Journal of biological chemistry* **287**, 14336-14348 (2012).
5. S. U. M. Vanninen *et al.*, Heterozygous junctophilin-2 (JPH2) p.(Thr161Lys) is a monogenic cause for HCM with heart failure. *PloS one* **13**, e0203422 (2018).
6. D. L. Beavers *et al.*, Mutation E169K in junctophilin-2 causes atrial fibrillation due to impaired RyR2 stabilization. *Journal of the American College of Cardiology* **62**, 2010-2019 (2013).
7. A. P. Quick *et al.*, Novel junctophilin-2 mutation A405S is associated with basal septal hypertrophy and diastolic dysfunction. *JACC. Basic to translational science* **2**, 56-67 (2017).
8. S. B. Seidelmann *et al.*, Application of Whole Exome Sequencing in the Clinical Diagnosis and Management of Inherited Cardiovascular Diseases in Adults. *Circulation. Cardiovascular genetics* **10** (2017).
9. A. Miura, H. Kondo, T. Yamamoto, Y. Okumura, H. Nishio, Sudden Unexpected Death of Infantile Dilated Cardiomyopathy with JPH2 and PKD1 Gene Variants. *International heart journal* **61**, 1079-1083 (2020).
10. Y. Matsushita *et al.*, Mutation of junctophilin type 2 associated with hypertrophic cardiomyopathy. *Journal of human genetics* **52**, 543-548 (2007).